

Simulation and optimization of bias magnetic field for giant magnetostrictive ultrasonic guided wave transducer

Hao Li^{a, b}, Zhonghu Li^{*,a, b}, Xinyu Zhang^c, Liqing Yang^{a, b}, Jinming Wang^{a, b}

^aSchool of Information Engineering, Inner Mongolia University of Science and Technology, Baotou 014010, China; ^bKey Laboratory of Solar Thermal and Wind Power Generation of Inner Mongolia Autonomous Region, Baotou 014010, China; ^cSchool of Mechanical Engineering, Inner Mongolia University of Science and Technology, Baotou 014010, China.

ABSTRACT

The corresponding relationship between magnetic induction intensity and GMM strain was analyzed theoretically. The finite element software COMSOL Multiphysics was used to select and compare the transducer, and the static simulation analysis of the bias magnetic field was carried out. Taking the axial magnetic induction intensity and magnetic field heterogeneity of GMM rod as optimization evaluation indexes, the optimal magnetic circuit design scheme was determined by optimizing the transducer shell material, the relative permeability of magnetic block and the structural parameters of permanent magnet. The two indexes were significantly improved and the magnetic leakage was reduced, and clear test results were obtained.

Keywords: Giant magnetostriction, Ultrasonic guided wave, Transducer, Bias magnetic field, Magnetic circuit optimization

1. INTRODUCTION

Giant magnetostrictive material (GMM) has the advantages of high driving accuracy, high mechanical and electrical conversion efficiency, fast response speed, large magnetostrictive coefficient, etc. The giant magnetostrictive ultrasonic guided wave transducer uses GMM rod to generate mechanical vibration under the bias magnetic field and high-frequency alternating driving magnetic field, so as to realize the conversion between electricity-magnetic field-mechanical energy^{1,2}. The mechanical vibration is loaded into the pipeline with defects to generate ultrasonic guided wave, which can be combined with the receiving transducer to complete the defect detection.

*Email: lizhonghu@imust.edu.cn

Yang X.L et al.³ conducted a simulation analysis on the giant magnetostrictive electrohydrostatic actuator (GMEHA) and compared the bias magnetic field provided by DC coil and permanent magnet. The experiment showed that the bias magnetic field provided by permanent magnet had a low displacement peak, but the difference was small and the heat dissipation was good. It can greatly improve the control accuracy and working time of GMEHA, and provide a reference for the selection of magnetic field bias mode in the subsequent research. Chen S et al.⁴ compared the open and closed state of the magnetic circuit and verified that the magnetic field in the GMM bar of the closed magnetic circuit has greater intensity, greater uniformity and smaller fluctuation range, and that the permanent magnet can provide a stable magnetic field to avoid the phenomenon of "frequency doubling". Liu Q et al.⁵ used the finite element software to optimize the magnetic circuit gap size of the giant magnetostrictive transducer. The results showed that the magnetic field strength and uniformity decreased with the increase of the gap, and the groove width of the optimal magnetic cylinder was determined through experiments. Yan H.B et al.⁶ compared the thickness, radius and other parameters of permanent magnets in the biased magnetic field with the magnetic field of the closed magnetic circuit, obtained the distribution uniformity of the axial magnetic field in the GMM rod, selected the best response parameter values, verified the corresponding relationship between the output displacement and the magnetic field uniformity, and further optimized the magnetic field uniformity. Gao X.H et al.⁷ used Ansoft Maxwell simulation software to design magnetic conductive end caps at both ends of magnetic circuits to suppress magnetic leakage. By changing the diameter and thickness of the end caps, the functional relationship between these two parameters and the maximum magnetic field intensity was compared and analyzed, and the end cap parameters at the maximum magnetic field intensity were obtained. Du G.X et al.⁸ built a test platform for the characteristics of giant magnetostrictive bars, which could measure the B-H curve and Young's modulus of GMM bars and other properties and parameters, providing feasible experimental support for the finite element simulation test.

According to the current research status, giant magnetostrictive transducers are mostly involved in machining, micro-displacement sensing system and other fields⁹⁻¹¹. While there are few reports on the application of giant magnetostrictive transducers to ultrasonic guided waves for defect detection. Due to the high frequency response required by ultrasonic detection, the magnetic field uniformity is required to be higher. So the study of bias magnetic field is of great significance.

2. STRUCTURE ANALYSIS AND MODEL ESTABLISHMENT OF TRANSDUCER

2.1 Structural analysis of transducer

Common giant magnetostrictive transducers are mainly composed of driving magnetic field, GMM rod, bias magnetic field, output rod and prestressed device. Figure 1 shows two models of giant magnetostrictive transducers with different structures. Figure 1 (a) shows the biased magnetic field provided by the DC coil. The magnetic field intensity of this structure can be adjusted by the current, but it is not suitable for long-term use due to its complex structure, large eddy current and high heat generated by the coil; The other is the bias magnetic field provided by the permanent magnet, as shown in Figure 1(b). The size of the bias magnetic field generated by this method is not adjustable, but it is more suitable for small transducers by taking advantage of the large magnetic product energy, relatively simple structure and low cost of the permanent magnet.

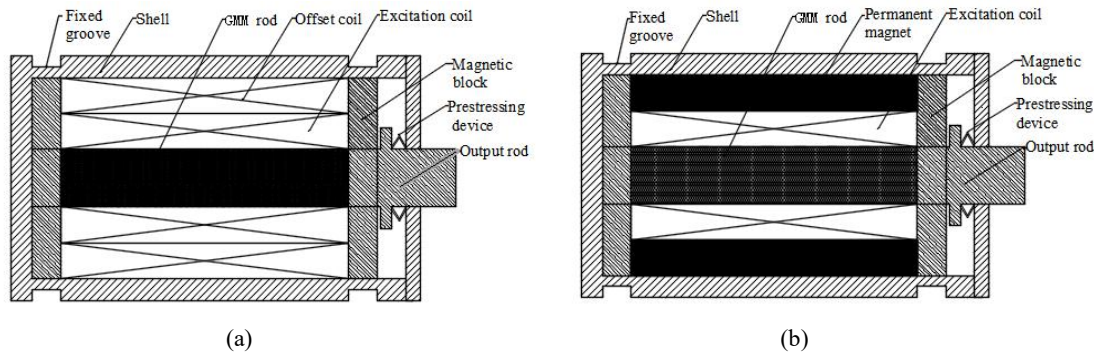


Figure 1. (a) Coil biased magnetic field transducer, (b) permanent magnet biased magnetic field transducer

Permanent magnet biased magnetic field can be divided into cylinder type and cylindrical type according to different structural forms, as shown in Figure 2. The selection of permanent magnet type affects the structure of magnetic circuit and the size and uniformity of magnetic induction intensity in GMM bar. Generally, the uniformity of cylindrical magnetic field is greater than that of cylindrical magnetic field. The selection and optimization of bias magnetic field are carried out through simulation and comparison test.

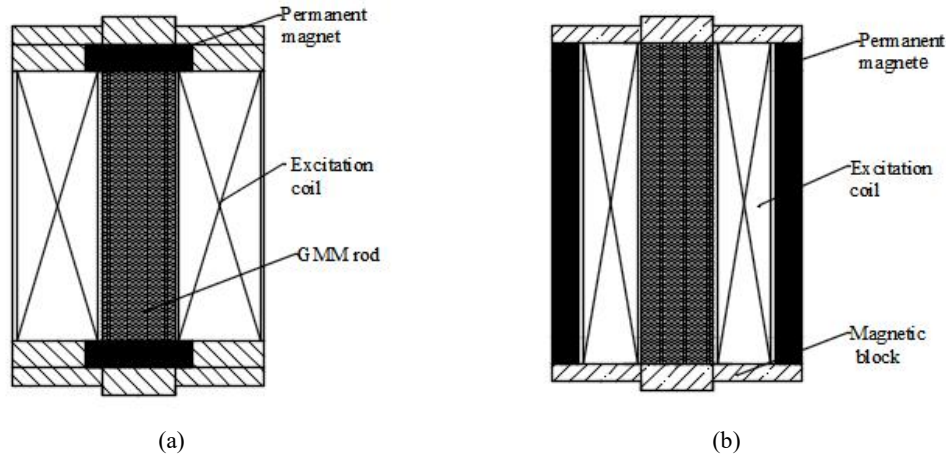


Figure 2. (a) Cylindrical permanent magnet ,(b)Cylinder permanent magnet

2.2 Theoretical analysis of the transducer

The magnetic field and external pressure of the GMM rod in the transducer change, resulting in magnetostrictive deformation and magneto-mechanical coupling effect.Changes in applied pressure will also cause magnetic field changes in magnetostrictive materials, thus generating mechanical-magnetic coupling effect. The constitutive relation of this effect under static magnetic field condition¹² is:

$$\lambda = \frac{\sigma}{E_y} + d_{33}H \quad (1)$$

$$B = d_{33}\sigma + \mu^\sigma H \quad (2)$$

Type: λ is material strain; d_{33} piezomagnetic coefficient; E_y is the elastic modulus; H is the magnetic field intensity; σ is the compressive stress of GMM bar; μ^σ is the relative permeability of the GMM bar under a given pressure. B is magnetic induction intensity.

According to Formula (1) and Formula (2), it can be obtained:

$$\lambda = \left(\frac{1}{E_y} - \frac{d_{33}}{\mu^\sigma} \right) \sigma + \frac{d_{33}}{\mu^\sigma} B \quad (3)$$

By the formula (3), on the assumption that d_{33}, E_y, μ^σ is constant, the quantitative σ for a specific value. The linear correspondence equation can be used to describe the relationship between the strain λ and the magnetic induction B of the magnetostrictive material. Therefore, the magnitude and uniformity of magnetic induction in the GMM rod will affect the magnitude of strain.

2.3 Transducer model establishment and analysis

The magnetostrictive module in COMSOL Multiphysics was used for modeling, and the magnetic field uniformity in GMM rod was analyzed according to different magnetic loops composed of different structures and materials. Firstly, the magnetic field uniformity was simulated and compared with the structural selection of two permanent magnets.As the transducer has an axisymmetric structure, two-dimensional modeling is conducted, as shown in FIG. 3.

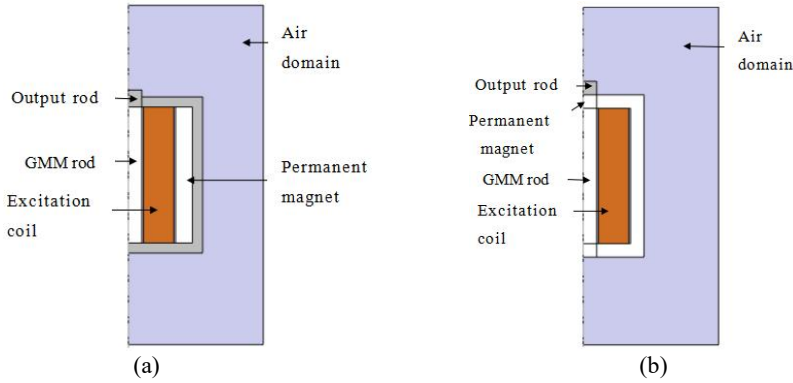


Figure 3.(a) Cylinder permanent magnet transducer, (b) Cylindrical permanent magnet transducer

The main material parameters in the model are shown in Table 1.

Table 1. Main material related parameters of the transducer model

Material	Electrical Conductivity (s/m)	Relative permeability
Copper	5.998×10^7	1
Pure Iron	1×10^7	2000
GMM Rod	1.66×10^6	7.5
NDFEB	6.25×10^5	1.05
Aluminum	3.03×10^7	1

Define ψ for magnetic field uniformity coefficient of uniformity is the higher the coefficient is small, the larger the coefficient that the magnetic induction intensity near 1 say more uneven. Where H_{\max} is the maximum axial or radial magnetic induction in the GMM bar and H_{\min} is the minimum axial or radial magnetic induction in the GMM bar. Then the coefficient ψ can be written as:

$$\psi = \frac{H_{\max} - H_{\min}}{H_{\max}} \times 100\% \quad (4)$$

The magnetic induction intensity distributions of two permanent magnets are shown in Figure 4. The field inequality coefficient of the cylindrical permanent magnet transducer is recorded as ψ_1 , and the cylindrical inequality coefficient is recorded as ψ_2 . The comparison of axial magnetic induction intensity of GMM rod is shown in Figure 4 (a), Calculated by the male type (4) can get $\psi_1 = 66.72\%$, $\psi_2 = 98.55\%$. It is proved that the magnetic field uniformity of the cylindrical transducer is obviously higher than that of the cylindrical permanent magnet transducer, and the magnetic induction intensity in the cylindrical transducer GMM rod is also greater than that in the cylindrical transducer GMM rod except near the two ends of the GMM rod.

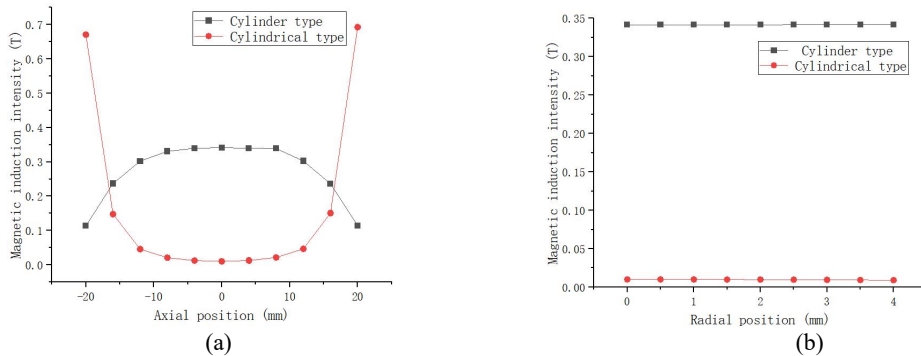


Figure 4.(a) Axial magnetic induction of GMM rod ,(b)GMM rod radial magnetic induction

As shown in FIG. 4 (b), the radial magnetic induction intensity at the center of GMM rods of the two structures does not change significantly, and the optimization focuses on the axial direction. According to Formula (4), the radial magnetic field inequality of cylindrical GMM rod is 0.15%, and that of cylindrical permanent magnet is 10.29%. The magnetic field uniformity of cylindrical permanent magnet is higher in both radial and axial direction than that of cylindrical permanent magnet, and the magnetic induction intensity generated by cylindrical permanent magnet in GMM rod is too small, which cannot meet the requirements of transducer on magnetic field intensity. The cylindrical permanent magnet is preferred to optimize the magnetic circuit design.

3. TRANSDUCER MAGNETIC CIRCUIT OPTIMIZATION

3.1 Transducer magnetic circuit design

The magnetic circuit design of the transducer directly affects its working performance. A good closed magnetic circuit can reduce magnetic leakage and make the magnetic induction intensity and uniformity conform to the linear working range of magnetostrictive materials.

(1) Selection of transducer shell material

The enclosure of the transducer can not only protect and support the internal components, but also act as a part of the magnetic circuit in the magnetic field to conduct the magnetic circuit or prevent magnetic leakage. First, the commonly used industrial pure iron is used as the transducer shell for analysis. As shown in Figure 5 (a), compared with the iron shell, the relative permeability of the GMM rod is lower, which makes most of the magnetic induction lines pass through the iron shell and form a closed magnetic loop with the permanent magnet, and only a small part passes through the GMM rod. When the aluminum shell is used, because the permeability of the aluminum shell is smaller than that of the GMM rod, the GMM rod, permanent magnet and output guide rod form a closed magnetic loop, as shown in Figure 5 (b). But at this time, the magnetic induction lines are mostly concentrated at the end of the permanent magnet and spread into the air outside the transducer after passing through the aluminum shell with low permeability, resulting in serious magnetic leakage phenomenon.

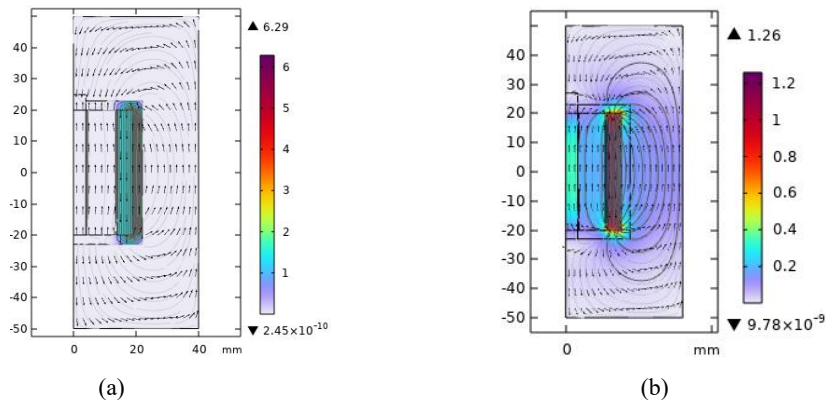


Figure 5.(a)Iron case magnetic induction wire, (b)Aluminum case magnetic induction wire

A magnetic leakage monitoring point was set at the external distance of the two shell models 30mm from the center of the GMM rod. The magnetic leakage caused by the two materials was numerically compared. The axial magnetic induction intensity of the point was 0.00077T when the iron shell was used, and the axial magnetic induction intensity of the middle point of the GMM rod was 0.0022T. The axial magnetic induction intensity at the monitoring point of the aluminum shell is 0.133T, and that at the middle point of the GMM rod is 0.342T, which also verifies the distribution of magnetic field lines in FIG. 5 and the correctness of the above analysis.

(2) Magnetic induction analysis of magnetic blocks with different relative permeability

Respectively choosing relative permeability is including, $\mu_r=2, 10, 200, 400, 800, 1500, 2000, 2500$ different material as permeability blocks is studied, the result is shown in figure 6(a), GMM rod axis to the magnetic induction intensity and permeability of material permeability increases with the strain of big trend, when relative permeability increased to more

than 200. The value of axial magnetic induction in GMM rod changes slowly with the increasing velocity of permeability. According to formula (4), the magnetic field unevenness generated by the above magnetic block is calculated respectively, as shown in Figure 6(b). When the relative permeability of the magnetic block is 2, the axial magnetic induction intensity in the GMM bar is still extremely uneven, reaching 49.77%. When the permeability reaches more than 800, the unevenness tends to be stable, almost does not change with the increase of the permeability, so choose the relative permeability of 2000, easy to process and cheap industrial pure iron as the magnetic block, GMM rod axial magnetic field unevenness of 10.98%.

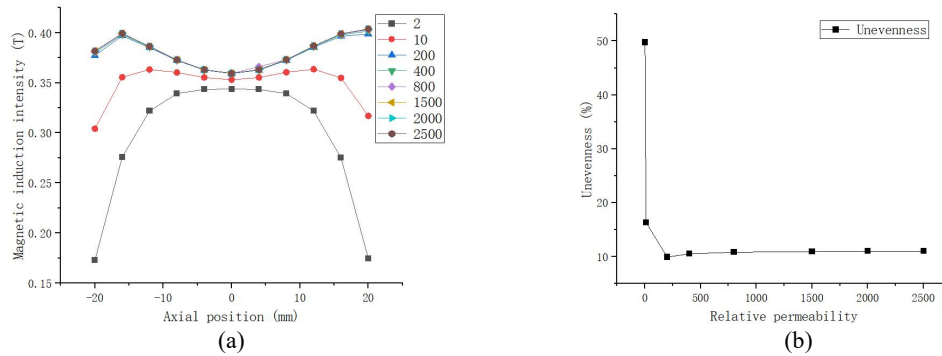


Figure 6.(a)Axial magnetic induction intensity of GMM bar with different permeability blocks . (b)Axial magnetic field unevenness of GMM bar with different materials.

(3) Influence of permanent magnet length on axial magnetic field uniformity of GMM rod

Taking the original length of 40mm shown in Figure 7 (c) as reference, the unevenness of the axial magnetic field in the GMM rod at the length of 32mm, 36mm and 44mm was discussed respectively. The results are shown in Figure 7 (a), (b) and (d). When the permanent magnet is smaller than 40mm, high permeability magnetic blocks with thickness of 2mm and 4mm are added to both ends of the permanent magnet. When the axial length of permanent magnet is greater than 40mm, the magnetic conductive block should be extended at both ends of the GMM rod for the purpose of reducing magnetic leakage in the magnetic circuit and increasing magnetic induction intensity.

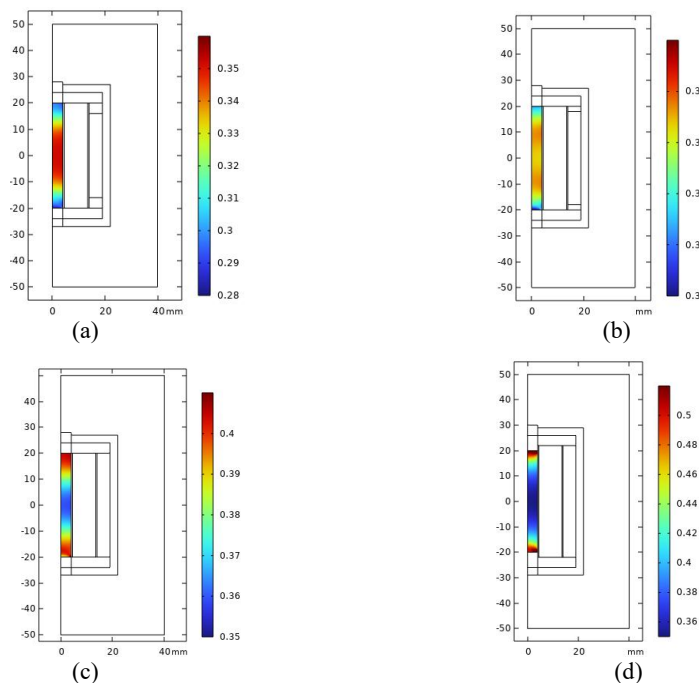


Figure 7. (a) Permanent magnet with 32mm length, (b) Permanent magnet with 36mm length, (c) Permanent magnet with 40mm length, (d) Permanent magnet with 44mm length

Combined with FIG. 7 and FIG. 8(a), the length of permanent magnet has a significant influence on the axial magnetic field in the GMM rod. When the length is less than 36mm, the magnetic induction intensity at both ends of the GMM rod is less than the center, and when the length is greater than 36mm, the magnetic induction intensity at both ends is greater than the center. FIG. 8 (b) shows the transformation trend of specific non-uniformity, in which the minimum value is 6.89% when the length is 36mm and the maximum non-uniformity is 32.36% when the length is 44mm. Therefore, it can be determined that the optimal length of permanent magnet is 36mm.

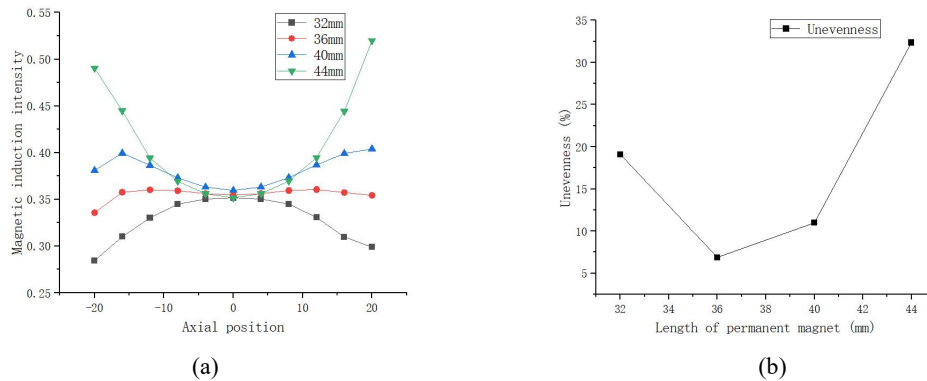


Figure 8. (a)Axial magnetic induction values in GMM rods of permanent magnets of different lengths,(b)Axial magnetic field unevenness of GMM rod with different permanent magnet lengths

3.2 Comparative analysis of transducer magnetic circuit optimization

Figure 9 (a) shows the overall optimized distribution of the transducer's bias magnetic field. Compared with the non-optimized state in Figure 5 (b), most of the magnetic induction lines generated by the permanent magnet enter the GMM rod through the magnetic conductive block, and the magnetic leakage is significantly reduced. The magnetic induction lines are evenly distributed at both ends of the GMM rod and the center point. Figure 9(b) shows the comparison curve before and after optimization. Before optimization, the magnetic field unevenness is 66.72%, and the mean magnetic induction intensity is 0.272T. After optimization, the non-uniformity is 6.89% and the mean magnetic induction intensity is 0.356T. The magnetic field uniformity and magnetic induction intensity were increased by 59.83% and 0.084T, respectively, and the two optimization indexes were improved.

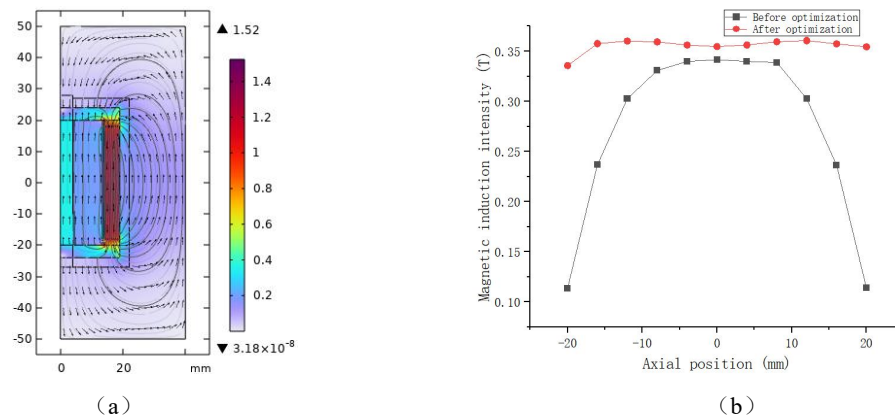


Figure 9. (a)Distribution of magnetic induction lines after optimization.(b) Comparison of axial magnetic induction intensity between optimized and original GMM rod.

4. CONCLUSION

In this paper, the characteristics of two magnetostrictive ultrasonic guided wave transducers with different biased magnetic field structures are compared. Based on the magnetostrictive theory under static magnetic field, the finite element software is used to conduct simulation research on the magnetostrictive ultrasonic guided wave transducers, and

the optimal biased magnetic field structure form is selected by numerical comparison of specific magnetic induction intensity and non-uniformity. The non-ferromagnetic material is determined as the transducer shell. The influence of the magnetic block on the overall magnetic induction line distribution of the transducer was studied. The variation trend of the axial magnetic field uniformity of the GMM bar with different permeability of the magnetic block was analyzed, and the material and arrangement of the magnetic block were determined. The axial magnetic field non-uniformity of the GMM bar was reduced to 10.98%. By changing the axial length of permanent magnet, the optimal structural size of permanent magnet is determined to be 36mm, and the magnetic field non-uniformity is further reduced to 6.89%, while the average magnetic field intensity is also increased by 0.084T, which verifies the effectiveness of this experiment.

ACKNOWLEDGMENTS

Project Research on pipeline defect identification and visualization method under complex working conditions based on ultrasonic guided wave and structured light vision(62161042) supported by National Natural Science Foundation of China and Research on methods for identifying minor defects in Hydrogen high-pressure pipelines based on helical guided wave(NJZY23074) supported by Scientific research project of colleges and universities in Inner Mongolia Autonomous Region.

REFERENCES

- [1] Liu, Y., Dang, X. A., Yang L. J., Improvement and motion analysis of powder laying device of direct metal Sintering rapid forming machine, *Hot Working Art*, (19):207-209 (2012).
- [2] Xue, G. M., He, Z. B., Li, D. W., Li, Y. L., Yang, C. S., Modeling of magnetic field Strength of Giant Magnetostrictive Rod and Coil Optimization Analysis[J]. *Nanotechnology and Precision Engineering*, 12(02):85-90 (2014).
- [3] Yang, X. L., Zhu, Y. C., Fei, S. S., et al., Magnetic Field Analysis and Optimization of Giant Magnetostrictive electrohydrostatic Actuator, *Journal of Aerospace Power*, 31(09): 2210-2217(2016).
- [4] Chen, S., Zhao, L. D., Zhou, J, et al., Magnetic Circuit Design and Simulation of Rare Earth Giant Magnetostrictive Transducer, *Machinery Design & Manufacture*, (02):43-46 (2018).
- [5] Liu, Q., Li, P. Y., Xu, G. Y., et al., Magnetic circuit optimization Design of isomogiant magnetostrictive ultrasonic transducer, *Journal of Beijing University of Aeronautics and Astronautics*, 45(8):1639-1645 (2019).
- [6] Yan, H. B., Gao, H., Niu, Y, et al., Magnetic Circuit Design and Simulation of Giant Magnetostrictive Actuator, *Machinery Design & Manufacture*, (02):242-246+251 (2022).
- [7] Gao, X. H., Liu, Y. G and Pei, Z. C., "Magnetic Circuit Optimization Design of Giant Magnetostrictive Actuator," *Journal of Harbin Institute of Technology*, 48(09):145-150(2016).
- [8] Du, G. X., Yang, X., Wei, Y. F, et al., Optimization and Experimental Study of Rare Earth Giant Magnetostrictive Bar Characteristics Test Platform, *Transactions of China Electrotechnical Society*, 36(18):3867-3875 (2021).
- [9] Li, P. Y., Liu, Q., Zhou, L. X., Design and analysis of giant Magnetostrictive ultrasonic Transducer, *Chinese Journal of Basic Science and Engineering*, 25(05):1065-1075 (2017).
- [10] Liu, J., Zhang, T. L., Wang, J. M, et al., Advances in Giant Magnetostrictive Materials and Their Applications, *Materials Advances in China*, 31(04):1-12+25 (2012).
- [11] Zhai, P., Xiao, B. H., He, K, et al., Compound Feedback Control of Giant Magnetostrictive Actuator and Its Application in Precision Machining of Variable Elliptic Pin Hole, *Optics and Precision Engineering*, 24(06):1389-1398 (2016). (In Chinese)
- [12] Tu, J. W., Liu, Z. F., Li, Z., Magnetic Circuit Optimization Design and Finite Element Analysis of Giant Magnetostrictive Actuator, *Journal of Chongqing University*, 44(04): 52-63 (2021).